Synthesis and Characterization of $Cubi_2o_4$ Nanoparticles and Evaluation of Its Antibacterial and Anticancer Activity

Ch.Jagadeesh, M.L.V.Prasanna.Ch, D.Anand Kumar, Ch.Sudhakar, B.B.V.Sailaja

Abstract: ***$CuBi_2O_4$ nanoparticles (NPs) were prepared by Co-precipitation strategy and portrayed by UV–noticeable spectroscopy, X-beam diffraction (XRD), Fourier Transform Infrared (FT-IR), Scanning Electron Microscope (SEM) and Energy Dispersive Spectroscopy (EDS) examination. The blended NPs were exceptionally steady, circular and crystallite size was determined as 68.29 nm. In addition, hydroxyl radicals have been recognized in the photocatalytic response blend by utilizing Terephthalic acid in photoluminescence testing method. The proficiency of antibacterial movement of $CuBi_2O_4$ NPs was assessed against Escherichia Coli (MTCC-443).The cytotoxicity action of $CuBi_2O_4$ NPs was assessed by Sulforhodamine B (SRB) measure against A549 lung malignant growth cell lines and affirmed that $CuBi_2O_4$ NPs have cytotoxicity action.***

Keywords: ***$CuBi_2O_4$ nanoparticles, photoluminescence, antibacterial activity, cytotoxicity activity, SRB Assay.***

I. INTRODUCTION

In recent years, metallic nano particles are cautiously being investigated and broadly considered as potential antimicrobials. These have incredible thought to analysts because of their potential innovative applications, for example, business merchandise: water treatment, sensors, biomedical, vitality, beautifying agents, medication and quality conveyance, and bio imaging gadgets [1–4]. All the more as of late, metal nanoparticles have gotten incredible significance for some innovative applications because of their little size and one of kind physical and synthetic properties. The use of nanomaterials in the medication conveyance frameworks has been explored for over twenty years achieving advance of measurements structures with improved remedial impacts and physicochemical attributes [5-6]. It is realized that the little nanoparticles have the most grounded bactericidal impact [7-9]. Metal nanoparticles with antimicrobial action when implanted and covered on to surfaces can discover tremendous applications in water treatment, manufactured materials, biomedical and medical gadgets [10-11]. The positive surface charge of the metal nano particles facilitates their binding to the negatively charged surface of the bacteria which may result in an enhancement of the bactericidal effect [12]. Several types of nano particles and their derivatives have received great attention for their potential antimicrobial effects. Metal nano particles such as Ag, silver oxide [13] Cerium oxide NPs increased oxidative stress and apoptosis in irradiated cancer cells, while protecting normal tissues [14-15].Titanium dioxide [16-18], silicon [19], copper oxide [20-22], zinc oxide [23-25], Au, calcium oxide [26] and magnesium oxide (MgO) [27] were identified to exhibit antimicrobial activity. In vitro studies revealed that metal nano particles inhibited several microbial species. Among all metal nano particles, CuO NPs have emerged as potential material due to their applications in catalysis, antimicrobial, antifungal, anticancer, and water treatment [28–30]. Copper oxide (CuO) nano particles have been of great interest due to its potential applications in many important fields of science and technology such as gas sensors, magnetic phase transitions, catalysts and superconductors [31-32]. The kind of the materials used for preparing the nano particles as well as the particle size were two important parameters that affected the resultant antimicrobial effectiveness [33-34].

In addition to antimicrobial activity, metal nanoparticles may target cancer cells [35]. Among different metal nanoparticles, copper oxide nanoparticles (CuO NPs) are widely used to attack cancer cells [36]. Hanagata et al. [37] showed the copper ions released from CuO NPs arrest the cell cycle, induced DNA damage and down regulated the proliferating cell nuclear antigen in lung epithelial A549 cells. Recently reported that *Ficus religiosa* leaf extract mediated CuO NPs potent anticancer activity in A549 lung cancer cells using cell proliferation, intracellular reactive oxygen species and mitochondrial membrane potential assay [38]. In the present study, we hypothesize that the $CuBi_2O_4$ NPs-induced antibacterial activities against Gram negative bacteria (E. coli) and anticancer activity in A549 lung cancer Cell lines also demonstrated.

II. MATERIALS AND METHODS

A. Synthesis of photocatalyst

In our previous work $CuBi_2O_4$ NPs were prepared by co-precipitation synthesis at 300°C [39]. Stoichiometric amounts of $Cu(NO_3)_2.3H_2O$ (LOBA CHEMIE PVT. Ltd) and $Bi(NO_3)_3.5H_2O$ (98% HIMEDIA) were dissolved in

Revised Manuscript Received on October 05, 2019

* Correspondence Author

Ch.Jagadeesh, Dept. of Inorganic and Analytical Chemistry, Andhra University,Visakhapatnam, India.

M.L.V.Prasanna.Ch Dept.of Inorganic and Analytical Chemistry, Andhra University, Visakhapatnam, India.

D.Anand Kumar, A.U. College of Pharmaceutical Sciences, Andhra University, Visakhapatnam, India.

Dr.Ch.Sudhakar, Asst.Professor Dept. of .Chemistry,Gitam (Deemed to be University), Visakhapatnam., India.

Dr.B.B.V.Sailaja*, Associate professor, Dept. of Inorganic and Analytical Chemistry, Andhra University,Visakhapatnam, India.

Ethylene Glycol separately by using magnetic stirrer. After completion of solubility two solutions were mixed with each other and heated at 50°C. By maintaining this temperature, 5N NaOH was added to maintain the P^H at 8.5. At this P^H the mixed precursors start react with each other and produced a blue color precipitate. This precipitate was washed a few times with refined water to totally evacuate the overabundance NaOH and the hasten was sifted and dried at 80 ºC in an air broiler. The dried powder was calcined at 300 ºC. The resultant impetus was grounded to a few hours to get fine powder and exposed to phase, micro structural, photo catalytic, antibacterial and anticancer investigations.

B. Characterization techniques

Diffractometer (PANalytical- X‟ Pert PRO, Japan) was used to identify phase purity of the resultant NPs at room temperature, using Nickel filtered Cu-Kα radiation (λ= 1.54059 Å), with a scan rate of 2° min^{-1}. SEM (JEOL-JSM-6610LV, Tokyo, Japan) was used for the micro structural investigation of the NPs. Shimadzu UV-visible spectrophotometer (UV-3600) between 200 to 800 nm range, was used to obtain UV–visible diffuse reflectance spectrum (UV-DRS) of the sample with dry pressed disk samples. Spectral grade $BaSO_4$ was used as reference in the UV-DRS.

C. Photo catalytic activity measurements

In our previous work photo catalytic activity of $CuBi_2O_4$ was studied with reference to degradation of Rose Bengal (RB) dye in presence of visible light. 50 mg of the catalyst was dispersed in 100ml of 10 ppm RB solution and the suspension was stirred for half an hour in the dark chamber to make sure adsorption/desorption equilibrium between dye solution and photo catalyst powder. The suspension was then treated with 400 wt metal halide lamp. At periodic time intervals, 5ml aliquots were pipetted and sifted through 0.45 micron Millipore filters to eliminate the suspended powder. The spectra as a function of irradiation and time were recorded using UV-Visible spectrophotometer (Schimadzu). The magnitude of photo degradation was calculated by using the following equation[39].

% of Photo degradation = $[(A_0-A_t)/A_0] \times 100$

where A_0 and A_t correspond to the initial absorbance and absorbance at time ‘t’ respectively.

D. Photoluminescence studies

100 ml of Pterpthalic acid (TPA) solution (0.25 mmol L^{-1} in 1 mmol L^{-1} NaOH solution) and 50 mg $CuBi_2O_4$ NPs were taken in a beaker. After stirring for 15 min in a dark chamber the above solution was irradiated by 400 w metal halide lamp for 45 min. The irradiated solution was centrifuged and the supernatant clear solution was used for photoluminescence measurements by using fluorescence spectrofluorometer (Flouromax 4) with the excitation wavelength of 315 nm.

E. Antibacterial studies

Agar-well diffusion technique was utilized to learn about antibacterial action of synthesized $CuBi_2O_4$ NPs [40-41] against bacterial strains Gram - ve organisms *Escherichia coli* (MTCC-443). Supplement Agar (High media-India) was set up by dissolving it in water and transferred into 100 mL conical flask and sterilized in an autoclave for 15 min at 121 °C 15 lbp. The disinfected media was transferred into pre-sterilized petri dishes and swabbed utilizing L-molded glass pole with 100 µL of 24 h developed stock culture of bacterial strain. The wells were made by sterile borer in the petri plates and various concentrations (200 µg/mL, 300 µg/mL and 400 µg/mL) of $CuBi_2O_4$ NPs were infused. The standard antibiotic Chloramphenicol (100 µg/mL) as positive control was tried against the bacterial pathogen, at that point the plates were incubated for 24 h at 37 °C. The distance across the zone of inhibition of each well was estimated in millimeter [42-43].

F. Cytotoxicity study of $CuBi_2O_4$ NPs against A549 cell line

Anticancer activity of prepared $CuBi_2O_4$ NPs was evaluated against A-549 cell line (lung) using **Sulforhodamine B (**SRB) assay. A-549 cell lines were grown in **Roswell Park Memorial Institute** (RPMI 1640) standard, consisting of 10% fetal bovine serum and 2 mM L-glutamine. For present screening test, cells were injected into 96 well microtiter plates in 100 µL at plating densities as appeared in the investigation subtleties above, contingent upon the multiplying time of individual cell lines. After cell injection, the microtiter plates were incubated for 24 h at 37° C, 5 % CO_2, 95 % air and 100 % relative moistness before the addition of test NPs.

$CuBi_2O_4$ NPs were at first solubilized in dimethyl sulfoxide at 100mg/ml and diluted to 1mg/ml with water and stored frozen before utilizing. During the NPs addition, an aliquot of frozen concentrate (1mg/ml) was defrosted and diluted to 100 µg/ml, 200 µg/ml, 400 µg/ml and 800 µg/ml with complete medium containing test NPs. Aliquots of 10 µl of these different NPs dilutions were added to the suitable microtiter wells which were already containing 90 µl of RPMI medium, resulting in the required final NPs concentrations that is 10 µg/ml, 20 µg/ml, 40 µg/ml and 80 µg/ml.

After the addition of $CuBi_2O_4$ NPs, plates were incubated at fixed conditions for 48 hours and assay was ended by the addition of cold TCA. Cells were fixed *in situ* by the calm addition of 50 µl of cold 30 % (w/v) TCA (final concentration, 10 % TCA) and incubated at 4°C for 1 h. The supernatant was discarded; the plates were washed 5 times with water and air dried. Sulforhodamine B (SRB) solution (50 µl) at 0.4 % (w/v) in 1 % acetic acid was added to each of the wells, and plates were incubated at room temperature for 20 minutes. After staining, unbound dye was back in place and the residual dye was eliminated by washing 5 times with 1 % acetic acid. The plates were air dried. Bound stain was consequently eluted with 10 mM trizma base, and the absorbance was read on plate reader at a wavelength of 540 nm with 690 nm respective wavelength. Percent of inhibition growth was calculated using below equation, and the concentration of $CuBi_2O_4$ NPs was needed to inhibit cell growth by 50% (IC50) value was calculated from the dose-response curve of cell line [43-44].

% Inhibition = 100 − (OD of the sample/OD of control) × 100.

III. RESULTS AND DISCUSSION

A. X-ray diffraction studies

The crystal structure and particle size of the obtained $CuBi_2O_4$ was analyzed by X-ray diffraction. **Fig. 1** shows the XRD pattern of the NPs. The XRD pattern of the $CuBi_2O_4$ can be indexed with 6 diffraction peaks at 27.8º (211), 29.6º (220), 33.1º (310), 44.9º(302), 46.5º(411), 52.71º(213) (JCPDS 72-0493),which suggests the presence of pure monoclinic phase of crystalline $CuBi_2O_4$ in the sample. The main diffraction peaks were selected to calculate the average crystallite size of $CuBi_2O_4$ NPs by using the Scherrer's formula. The calculated average size of $CuBi_2O_4$ nano particles by using Scherrer's formula **(Crystallite size Dp = K λ / (β cos Θ))** is 68.29 nm.

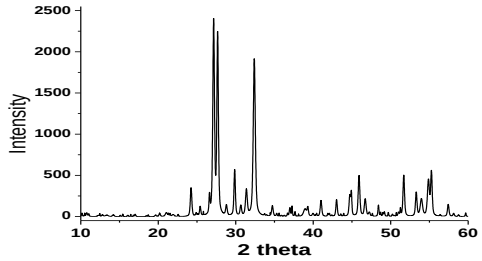

Fig.1. X-ray diffraction patterns of $CuBi_2O_4$.

B. UV–Vis diffuse reflectance studies

The UV–visible diffuse reflectance spectrum of monoclinic $CuBi_2O_4$ prepared at 300 ºC was measured as shown in **Fig.2.** It can be seen that the absorption wavelength boundary of $CuBi_2O_4$ is extensive very much toward visible light and its absorption intensity is also to a great extent improved. $CuBi_2O_4$ has high absorption in the wavelength range of 300–800 nm. This shows that the prepared sample absorbs both UV and visible light quite well, which is improved than that of TiO2. So the development rate of electron–hole pairs on the photo catalyst surface also goes up highly by visible light irradiation. Fig.2. shows that the synthesized $CuBi_2O_4$ shows an absorption at 489.502333 nm, which relates to band gap energy of 2.61 eV. This value is very less than that of TiO_2 (3.2 eV) and thus the as prepared CuBi2O4 sample can be foretold to be a fulfilling visible light active photo catalyst.

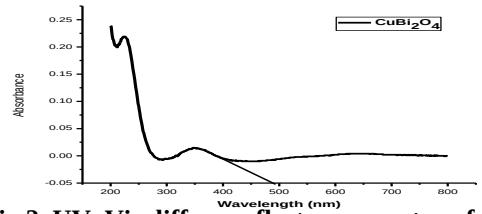

Fig.2. UV–Vis diffuse reflectance spectra of $CuBi_2O_4$

C. Micro structural investigation studies

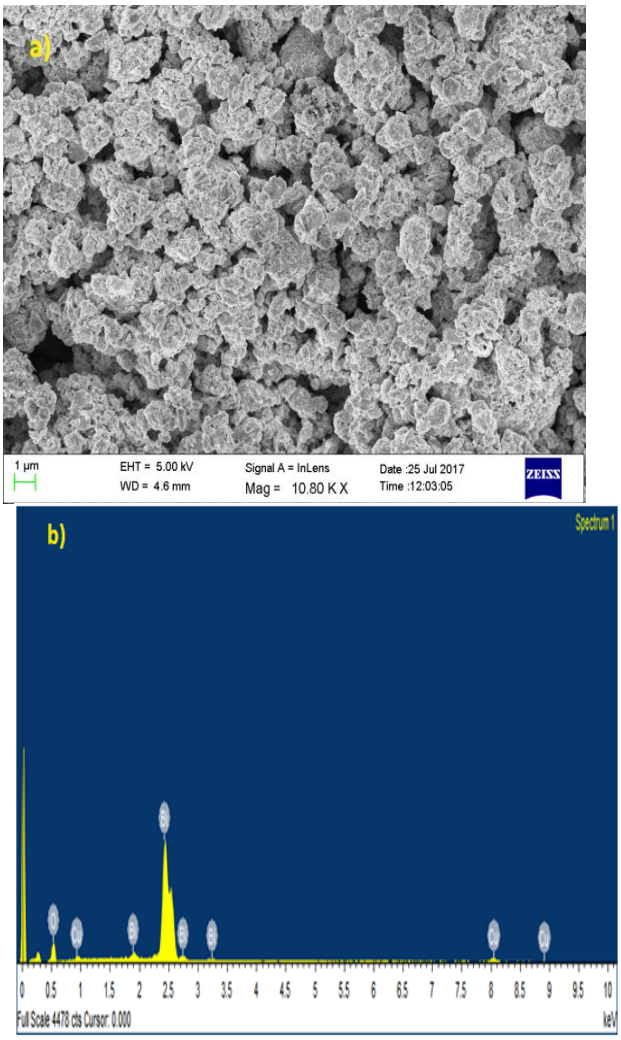

Fig.3. a) SEM image and b) EDS spectra of $CuBi_2O_4$

The micro structures of the prepared samples were studied by SEM analysis which can be observed from **Fig.3.a).** The SEM image shows that the photo catalyst contains a huge number of hierarchical nanostructures like sub micro-flowers with the size less than 100 nanometers and 2-dimensional crystalline nano particles. These NPs show agglomerated morphology due to the extremely fine nature of the NPs. EDS analysis of peak areas can observe in **Fig.3.b)**. EDS spectrum shows that the sample was composed with copper (Cu), bismuth (Bi) and oxygen (O) elements. According to the EDS data, the elemental percentages of Cu, Bi and O in $CuBi_2O_4$ are listed in **Table.1**. The quantifications ratio of Cu:Bi:O is 1:1.97:4.19. This atomic ratio of Cu:Bi:O is closer to 1:2:4, which nearly agrees with the stoichiometric composition of $CuBi_2O_4$. This result is reliable with the XRD pattern shown above.

Table.1.The atomic percentage (mol %) of Cu, Bi and O in $CuBi_2O_4$.

Compound	Atomic percentage (mol %)		
	Cu	***Bi***	***O***
$CuBi_2O_4$	1	1.97	4.19

D. FT-IR studies

The IR spectra of the calcined powder of $CuBi_2O_4$

shown in **Fig.4**. The spectrum is complex due to the presence of excessive organic compounds. The broad one around 700 ~ 400 cm^{-1} emerges from the bismuth-oxygen (Bi-O) bond vibration. The absorption band at 866 cm^{-1} shows the symmetric stretching of Bi-O bond. Bending vibrations of Cu-O at 574.79 supports monoclinic structure of the catalyst. Stretching frequencies at 478.36 belongs to Cu-O bond.

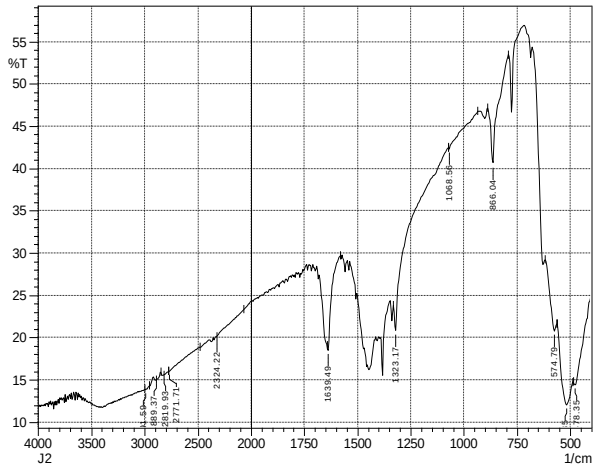

Fig. 4. FT-IR spectrum of $CuBi_2O_4$.

E. Photoluminescence studies

In order to confirm the generation ˙OH free radicals during irradiation of $CuBi_2O_4$, photo luminescence spectroscopy was used with pterpthalic acid (TPA) as a probe molecule. TPA combines preferentially with ˙OH to form hydroxy terpthalic acid (HTPA) which shows a characteristic luminescence peak at 422 nm. **Fig.5.** depicts photoluminescence spectra for $CuBi_2O_4$+TPA prior to and after irradiation. Intense luminescence peak after irradiation confirms formation of ˙OH free radicals due to irradiation.

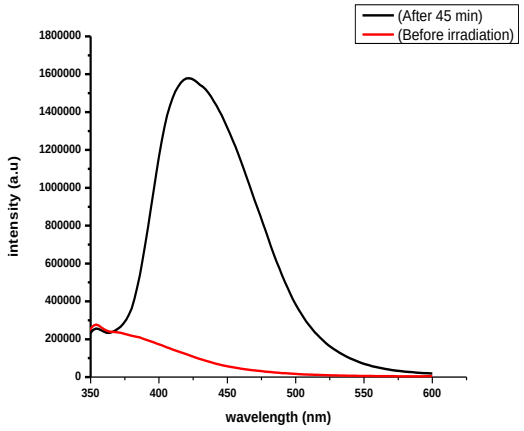

Fig.5. Photoluminescence spectra for $CuBi_2O_4$+TPA prior to and after irradiation for 45 minutes.

F. Antibacterial studies

The antibacterial activity of $CuBi_2O_4$ NPs was implemented by Agar-well diffusion technique against *Escherichia coli* (MTCC-443) at different concentration of $CuBi_2O_4$ NPs starting from 100 µg/mL, 200 µg/mL, 300 µg/mL and control chloramphenicol-300 µg/mL. The anti bacterial petri plates are showed in **Fig.6.** The bacterial growth of zone diameter was determined and the results are placed in **Table 2**. The activity results showed that (300 µg/ml) is the suitable concentration for the zone of inhibition of bacterial growth which is measured as 30 mm. This value is nearly closer to the control value 30 mm. Hence, $CuBi_2O_4$ NPs are having highest anti bacterial activity. This zone of inhibition of bacterial growth with the catalyst may be due to the formation of e−/h+ pairs on the surface of the catalyst when treated with visible light. The e−/h+ pairs can act as a strong oxidizing agent and the excited electron can react with adsorbed oxygen and convert it into super oxide radicals which in turn produce ˙OH radicals. Then these e−/h+ pairs and ˙OH radicals both can act as oxidizing agents which can deteriorate the protein coat of bacteria and leads to the inhibition of the organism's growth. During the photo catalysis, the formation of h+ and ˙OH can be detected by utilizing scavenging reagents [42].

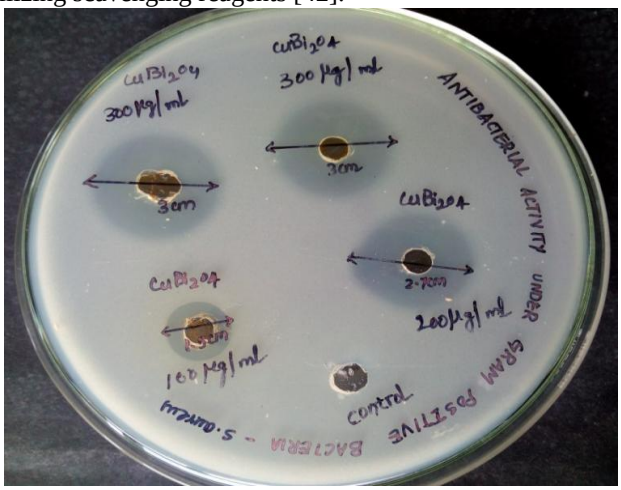

Fig.6. Zone of inhibition of $CuBi_2O_4$ NPs against *Escherichia coli* (MTCC-443)

Table 2 The zone of inhibition of $CuBi_2O_4$ nano particles against *Escherichia coli* (MTCC-443)

Microorganism	Zone of inhibition /mm			
	***100* µg/ml**	***200* µg/ml**	***300* µg/ml**	**Standard (Chloramphenicol) 100 µg/ml**
Escherichia coli (MTCC-443)	15	27	30	30

G. Cytotoxicity study of $CuBi_2O_4$ NPs against A549 cell line

The effect of $CuBi_2O_4$ NPs on the viability of A549 cells was analyzed by utilizing SRB assay [45-46]. The microscopic images of A549 cells treated with $CuBi_2O_4$ NPs before and after treating the cell culture after 48h and are shown in **Fig.7**. Cell viability of A549 deteriorates with rising dose of $CuBi_2O_4$ NPs. The amount of $CuBi_2O_4$ NPs necessary to lower the viability of A549 cells to 50% of the early population was 71.8 µg/ml and was marked as IC50 which can observe in graph **Fig.8**. So $CuBi_2O_4$ NPs can be used in biomedical research application depending on the calculated IC50 value. The cytotoxicity of $CuBi_2O_4$ NPs is due to the active copper ions with the functional groups of intracellular proteins, as well as with the phosphate groups in DNA and nitrogen bases [47-48]. Extended physical contact of $CuBi_2O_4$ NPs and A549 cells may bring an increase cytotoxicity, apoptosis, production of reactive

oxygen species (ROS) and mitochondrial damage, which may be easily included in cellular oxidative stress [43]. Drugs used in cancer therapy increases penetrability and withholding effect, passively attacking the leaky vasculature of the tumor cells, since the cancer cells do not have a sturdy vasculature system compared to that of ordinary cells[49]. Accordingly, the penetration of the drugs is easier and at last destructs the cancer cells, however sometimes it penetrates into the ordinary cells and cause toxic effects [50]. The detailed mechanism of cytotoxicity of $CuBi_2O_4$ NPs will be analyzed in our further work.

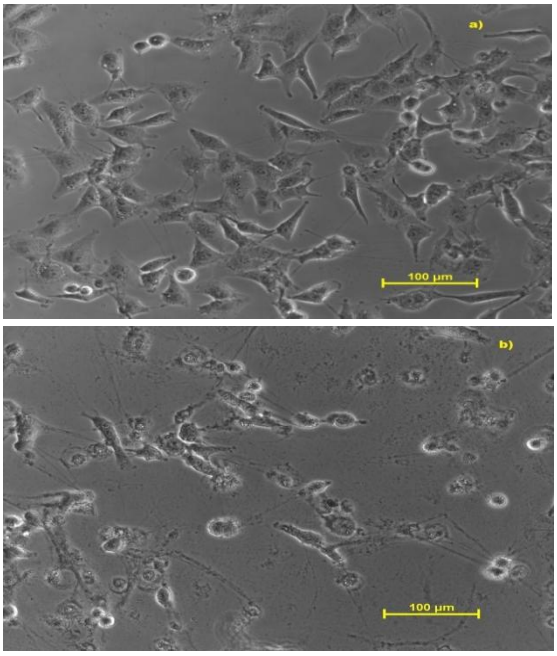

Fig.7. Microscopic pictures of A549 cells (a) before exposure, (b) after exposure to $CuBi_2O_4$ NPs after 48 h in cell culture.

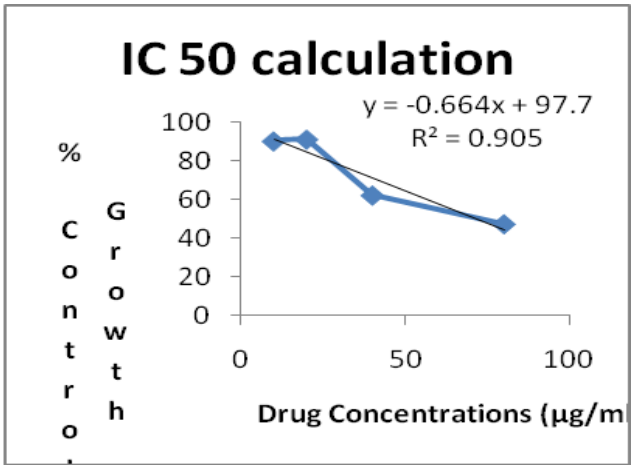

Fig.8. Dose-dependent effect of $CuBi_2O_4$ NPs over the cell viability using SRB assay.

IV. CONCLUSIONS

We have synthesized $CuBi_2O_4$ NPs by using simple co-precipitation method. The synthesized catalysts characterized by various analytical techniques. FT IR spectra established the presence of Cu–O, Bi-O bonding and XRD patterns exposed the monoclinic phase of $CuBi_2O_4$. UV–vis spectra of the $CuBi_2O_4$ nano particles open characteristic absorption peak at 489.502333 nm. SEM and XRD studies definite spherical shape and crystallite size of the prepared nano particles. EDX analysis established the elemental composition of $CuBi_2O_4$. The catalyst showed strong antibacterial activity against *Escherichia coli* (MTCC-443). The synthesized nano particles showed significant cytotoxicity against the lung cancer cell lines (A549) without significant effect against the ordinary cells with regard to standard drug cisplatin. The anticancer activity of $CuBi_2O_4$ usually has been endorsed to the decay of cancer cell outer membranes by reactive oxygen species (ROS), first and foremost hydroxyl radicals (OH), which takes to phospholipid peroxidation and eventually cell death. In our previous and present study, $CuBi_2O_4$ NPs can be used as a winning catalyst for degradation of Rosebengal dye and as antibiotic against gram -ve (*E. coli*) and against proliferation of A549 (Human lung cancer) cell line. Additional analysis is needed to verify its effect on various cancer cells.

ACKNOWLEDGMENT

The authors recognize the DST-FIST and UGC-SAP DRS-1, Department of Inorganic and analytical chemistry, Andhra University for relevant equipment. The authors like to thank University Grant Commission (UGC), New Delhi, INDIA, for their economical support of this research under RGNF.No."F1-17.1/2016-17/RGNF-2015-17-SC-AND-631 4/(SA-lll/Website)".

REFERENCES

1. B. Kumar, S. Kumari, L. Cumbal, A. Debut, Lantana camara berry for the synthesis of silver nanoparticles, Asian Pac. J. Trop. Biomed. 5 (2015) 192–195.
2. Q.H. Tran, V.Q. Nguyen, A.-T. Le, Silver nanoparticles: synthesis, properties, toxicology, applications and perspectives, Adv. Nat. Sci.: Nanosci. Nanotechnol. 4(2013) 033001.
3. M. Ahamed, M.S. AlSalhi, M.K.J. Siddiqui, Silver nanoparticle applications and human health, Clin. Chim. Acta. 411 (2010) 1841–1848.
4. M.A. Albrecht, C.W. Evans, C.L. Raston, Green chemistry and the health implications of nanoparticles, Green Chem. 8 (2006) 417.
5. K. Adibkia, Y. Javadzadeh, S. Dastmalchi, G. Mohammadi, F.K. Niri, M. Alaei-Beirami, Naproxen–eudragit RS100 nanoparticles: Preparation and physicochemical characterization,Colloids Surf. B 83 (2011) 155–159.
6. A. Sabzevari, K. Adibkia, H. Hashemi, A. Hedayatfar, N. Mohsenzadeh, F. Atyabi, M.H. Ghahremani, R. Dinarvand, Polymeric triamcinolone acetonide nanoparticles as anew alternative in the treatment of uveitis: In vitro and in vivo studies, Eur. J.Pharm. Biopharm. 84 (2013) 63–71.
7. C. Buzea, I.I. Pacheco, K. Robbie, Nanomaterials and nanoparticles: sources and toxicity, Biointerphases 2 (2007) MR17–MR71.
8. A. Besinis, T. De Peralta, R.D. Handy, The antibacterial effects of silver, titaniumdioxide and silica dioxide nanoparticles compared to the dental disinfectant chlorhexidine on Streptococcus mutans using a suite of bioassays, Nanotoxicology 8 (2014) 1–16.
9. O. Fellahi, R.K. Sarma, M.R. Das, R. Saikia, L. Marcon, Y. Coffinier, T. Hadjersi, M. Maamache, R. Boukherroub, The antimicrobial effect of silicon nanowires decorated with silver and copper nanoparticles, Nanotechnology 24 (2013) 495101.
10. Dou, Y., Han, J., Wang, T., Wei, M., Evans, D.G., and Duan, X., 2012. Langmuir, 28, 9535–9542.
11. Roslan, M.A.M., Mohamad, M.A.N., Omar, S.M., 2017. High-Quality Dna From Peat Soil for Metagenomic Studies: A Minireview On Dna Extraction Methods. Science Heritage Journal,1(2), 1-7.
12. J.T. Seil, T.J. Webster, Antimicrobial applications of nanotechnology: methods and literature, Int. J. Nanomedicine 7 (2012) 2767–2781.
13. A.M. Allahverdiyev, E.S. Abamor, M. Bagirova, M. Rafailovich, Antimicrobial effects of TiO2 and Ag2O nanoparticles against drug-resistant bacteria and leishmania parasites, Future Microbiol 6 (2011) 933–940.
14. Colon, J.; Hsieh, N.; Ferguson, A.; Kupelian, P.; Seal, S.; Jenkins,

D.W.; Baker, C.H. Cerium oxide nanoparticles protect gastrointestinal epithelium from radiation-induced damage by reduction of reactive oxygen species and upregulation of superoxide dismutase 2. Nanomedicine 2010, 6,698–705.
15. Tarnuzzer, R.W.; Colon, J.; Patil, S.; Seal, S. Vacancy engineered ceria nanostructures for protection from radiation-induced cellular damage. Nano Lett. 2005, 5, 2573–2577.
16. Zhang, A.P.; Sun, Y.P. Photocatalytic killing effect of TiO2 nanoparticles on Ls- 174-t human colon carcinoma cells. World J. Gastroenterol. 2004, 10, 3191–3193.
17. Thevenot, P.; Cho, J.; Wavhal, D.; Timmons, R.B.; Tang, L. Surface chemistry influences cancer killing effect of TiO2 nanoparticles. Nanomedicine 2008, 4, 226–236.
18. Seo, J.W.; Chung, H.; Kim, M.Y.; Lee, J.; Choi, I.H.; Cheon, J. Development of water soluble single-crystalline TiO2 nanoparticles for photocatalytic cancer-cell treatment. Small 2007, 3,850–853.
19. Meng, H.; Wang, M.; Liu, H.; Liu, X.; Situ, A.; Wu, B.; Ji, Z.; Chang, C.H.; Nel, A.E. Use of a lipid-coated mesoporous silica nanoparticle platform for synergistic gemcitabine and paclitaxel delivery to human pancreatic cancer in mice. ACS Nano 2015, 9, 3540–3557.
20. Zhang, X.; Wang, G.; Liu, X.; Wu, J.; Li, M.; Gu, J.; Liu, L.; Fang, B. Different CuO nanostructures:Synthesis, caracterization, and applications for glucose sensors. J. Phys. Chem. C 2008, 112,16845–16849.
21. Cioffi, N.; Torsi, L.; Ditaranto, N.; Tantillo, G.; Ghibelli, L.; Sabbatini, L.; Bleve-Zacheo, T.;D'Alessio, M.; Zambonin, P.G.; Traversa, E. Copper nanoparticle/polymer composites with antifungal and bacteriostatic properties. Chem. Mater. 2005, 17, 5255–5262.
22. Wang, Y.; Zi, X.Y.; Su, J.; Zhang, H.X.; Zhang, X.R.; Zhu, H.Y.; Li, J.X.; Yin, M.; Yang, F.;Hu, Y.P. Cuprous oxide nanoparticles selectively induce apoptosis of tumor cells. Int. J. Nanomed.2012, 7, 2641–2652.
23. Wahab, R.; Dwivedi, S.; Umar, A.; Singh, S.; Hwang, I.H.; Shin, H.S.; Musarrat, J.;Al-Khedhairy, A.A.; Kim, Y.S. ZnO nanoparticles induce oxidative stress in Cloudman S91 melanoma cancer cells. J. Biomed. Nanotechnol. 2013, 9, 441–449.
24. Wahab, R.; Kaushik, N.K.; Kaushik, N.; Choi, E.H.; Umar, A.; Dwivedi, S.; Musarrat, J.;Al-Khedhairy, A.A. ZnO nanoparticles induces cell death in malignant human T98G gliomas, KB and non-malignant HEK cells. J. Biomed. Nanotechnol. 2013, 9, 1181–1189.
25. Wahab, R.; Siddiqui, M.A.; Saquib, Q.; Dwivedi, S.; Ahmad, J.; Musarrat, J.; Al-Khedhairy, A.A.;Shin, H.S. ZnO nanoparticles induced oxidative stress and apoptosis in HepG2 and MCF-7 cancer cells and their antibacterial activity. Colloids Surf. B 2014, 117, 267–276.
26. O. Yamamoto, T. Ohira, K. Alvarez, M. Fukuda, Antibacterial characteristics of CaCO3–MgO composites, Mater. Sci. Eng. B 173 (2010) 208–212.
27. T. Jin, Y. He, Antibacterial activities of magnesium oxide (MgO) nanoparticles against foodborne pathogens, J. Nanoparticle Res. 13 (2011) 6877–6885.
28. Hanagata N, Zhuang F, Connolly S, Li J, Ogawa N, XuM(2011) Molecular responses of human lung epithelial cells to the toxicity of copper oxide nanoparticles inferred from whole genome expression analysis. ACS Nano 5:9326–9338
29. Sankar R, Ravikumar V (2014) Biocompatibility and biodistribution of suberoylanilide hydroxamic acid loaded poly (DL-lactide-co-glycolide) nanoparticles for targeted drug delivery in cancer. Biomed Pharmacother 68:865–871
30. Sun T, Yan Y, Zhao Y, Guo F, Jiang C (2012) Copper oxide nanoparticles induce autophagic cell death in A549 cells.PLoS ONE 7:e43442
31. Das, T.K., and Prusty, S., 2012. Review on Conducting Polymers and Their Applications. Polymer-Plastics Technology and Engineering, 51 (14), 1487-1500.
32. Razali, A., Zuraidah, M.A., John, B.A., Kamaruzzaman, Y., 2017. Cytotoxicity on Mcf7 Cell Lines Exposed to An Extract Of The Jacalin From Jackfruit Seed. Science Heritage Journal,1(2), 14-16.
33. J.T. Seil, T.J. Webster, Antimicrobial applications of nanotechnology: methods and literature, Int. J. Nanomedicine 7 (2012) 2767–2781.
34. K. Adibkia, M. Alaei-Beirami, M. Barzegar-Jalali, G. Mohammadi, M.S. Ardestani, Evaluation and optimization of factors affecting novel diclofenac sodium-eudragit RS100 nanoparticles, Afr. J. Pharm. Pharmacol. 6 (2012) 941–947.
35. Sankar R, Ravikumar V (2014) Biocompatibility and biodistribution of suberoylanilide hydroxamic acid loaded poly (DL-lactide-co-glycolide) nanoparticles for targeted drug delivery in cancer. Biomed Pharmacother 68:865–871
36. Sun T, Yan Y, Zhao Y, Guo F, Jiang C (2012) Copper oxide nanoparticles induce autophagic cell death in A549 cells. PLoS ONE 7:e43442
37. Hanagata N, Zhuang F, Connolly S, Li J, Ogawa N, XuM(2011) Molecular responses of human lung epithelial cells to the toxicity of copper oxide nanoparticles inferred from whole genome expression analysis. ACS Nano 5:9326–9338.
38. Sankar R, Maheswari R, Karthik S, Shivashangari KS, Ravikumar V (2014) Anticancer activity of Ficus religiosa engineered copper oxide nanoparticles. Mater Sci Eng C Mater Biol Appl 44:234–239
39. Jagadeesh Ch., Suresh P and Sailaja B.B.V (2017) 'Photocatalytic properties of CuBi2O4 prepared by the co-precipitation method:Degradation of rose bengal and possible reaction mechanism under visible light irradiation', International Journal of Current Advanced Research, 06(12), pp. 8605-8610. DOI: http://dx.doi.org/10.24327/ijcar.2017.8610.1392
40. A.W. Bauer, W.M. Kirby, J.C. Sherris, M. Turck, Am. J. Clin. Pathol. 45 (1966) 493–496.
41. Salama, M.H., Marraiki, N., 2015. Antimicrobial activity and phytochemical analyses of Polygonum aviculare L. (Polygonaceae), naturally growing in Egypt, Saudi. J. Bio. Sci.17, 57–63.
42. K.V. Divya Lakshmi, T. Siva Rao J. Nanosci. Tech. - Volume 4 Issue 5 (2018) 555–559
43. Mebrahtu Hagos Kahsaya,c, Dharmasoth RamaDevib, Y. Pavan Kumara,B.Sathish Mohana, Aschalew Tadessea,d, Gangarao Battub, K. Basavaiaha, OpenNano 3 (2018) 28–37
44. N. Hattori, T. Sakakibara, N. Kajiyama, T. Igarashi, M. Maeda, S. Murakami, Enhanced microbial biomass assay using mutant luciferase resistant to benzalkonium chloride, Anal. Biochem. 319 (2003) 287–295.
45. Vanicha Vichai and Kanyawim Kirtikara. Sulforhodamine B colorimetric assay for cytotoxicity screening Nature Protocols 1, - 1112 - 1116 (2006)
46. Skehn, P.; Storeng, R.; Scudiero, A.; Monks, J.; McMohan, D.; Vistica, D.; Jonathan, T. W.; Bokesch, H.; Kenney, S.; Boyd, M. R. New colorimetric cytotoxicity assay for anticancer drug screening J. Natl. Cancer Inst. 1990, 82, 1107.
47. Cioffi, N.; Torsi, L.; Ditaranto, N.; Tantillo, G.; Ghibelli, L.; Sabbatini, L.; Bleve-Zacheo, T.;D'Alessio, M.; Zambonin, P.G.; Traversa, E. Copper nanoparticle/polymer composites with antifungal and bacteriostatic properties. Chem. Mater. 2005, 17, 5255–5262.
48. Wang, Y.; Zi, X.Y.; Su, J.; Zhang, H.X.; Zhang, X.R.; Zhu, H.Y.; Li, J.X.; Yin, M.; Yang, F.;Hu, Y.P. Cuprous oxide nanoparticles selectively induce apoptosis of tumor cells. Int. J. Nanomed.2012, 7, 2641–2652.
49. Dilaveez Rehanaa,b, D. Mahendirana, R. Senthil Kumarc, A. Kalilur Rahimana,Biomedicine & Pharmacotherapy 89 (2017) 1067–1077.
50. E. Blanco, C.W. Kessinger, B.D. Sumer, J. Gao, Multifunctional micellar nanomedicine for cancer therapy, Exp. Biol. Med. 234 (2009) 123–131.

AUTHORS PROFILE

Ch.Jagadeesh, Dept. of Inorganic and Analytical Chemistry, Andhra University,Visakhapatnam, India

PUBLICATIONS:

1. Jagadeesh Ch., Suresh P and Sailaja B.B.V**;** Photocatalytic properties of $CuBi_2O_4$ prepared by the Co-precipitation method: Degradation of Rose Bengal and possible reaction mechanism under visible light irradiation. International Journal of Current Advanced Research.Volume 6; Issue 12; December 2017; Page No: 8605-8610.

2. Jagadeesh Ch., Sailaja B.B.V**;** Photocatalytic degradation of Methylene Blue dye using $CuBi_2O_4$ and effect of various operational parameters; International Journal of scientific research and reviews. Volume 8; Issue 1; March 2019; Page No: 3259-3273.

3. Jagadeesh Ch., Sailaja B.B.V**;** Photocatalytic degradation of Rhodamine B dye using $CoBi_2O_4$ nanocatalyst and effect of various operational parameters; Cikitusi Journal of Multidisciplinary Research. Volume 6; Issue 4; April 2019; Page No: 97-107.

M.L.V.Prasanna.Ch Dept.of Inorganic and Analytical Chemistry, Andhra University, Visakhapatnam, India.

D.Anand Kumar, A.U. College of Pharmaceutical Sciences, Andhra University, Visakhapatnam, India

Dr.Ch.Sudhakar, Asst.Professor, Dept. of Chemistry, GITAM (Deemed to be University), Visakhapatnam., India.

PUBLICATIONS:

1. Estimation of iron in pharmaceutical samples-A solvent extraction study **International Journal of Chem Tech Research,** 3 (2), pp. 703-707. (2011).
2. Studies on the solvent extraction of iron (III) with Tri-iso-octylamine from aqueous mineral acid solutions. **Oriental Journal of Chemistry,** 28 (4), pp. 1785-1790. (2012).
3. Influence of silico manganese slag on mechanical and durability properties of concrete **International Journal of Civil Engineering and Technology,** 9 (7), pp. 1597-1604. (2018).

Dr.B.B.V.Sailaja*, Associate professor, Dept. of Inorganic and Analytical Chemistry, Andhra University,Visakhapatnam, India.
E.mail: sailajabbv.chem@gamil.com

PUBLICATIONS:

1. B.B.V.Sailaja, Tesfahun Kebede, G.S.raju,M.S.Prasada Rao;Thermal decomposition of ammonium dioxodiaquaperoxyoxalato uranate(VI)Hydrate; **Thermochimica acta** 386, 51(2002).
2. M. Ramanaiah and B.B.V. Sailaja; pH-metric Investigation on Binary Complexes of Pb(II), Cd(II) and Hg(II) with maleic acid In SLS-Water Mixtures; **J. Indian Chem. Soc**., 2014(April), 91, 639-645.
3. V. Ashok Chakravarthy, B. B. V. Sailaja
Method Development and Validation of Assay and Dissolution Methods for the estimation of Daclatasvir in Tablet Dosage Forms by Reverse Phase HPLC; European Journal of Pharmaceutical and Medical Research; Volume 3, Issue 7, July 2016; Page No: 356-364